Pyroconvection Scenarios for Premier – Impact Study

We document the data and methods used to quantify surface fire emissions with three fires that resulted in significant pyroconvection, which we selected as part of the PREMIER impact study. These scenarios will be used as input for a high-resolution non-hydrostatic GEM-AQ runs.

**Theory**

Emission *E* of trace gas (kg/unit time):

$$E = mcfA,$$

where *m* is the fuel load (kg/m$^2$), *f* is the mass fraction of the trace gas emitted per amount of the dry fuel consumed (kg/kg), *c* is the combustion efficiency (i.e. how much of the fuel is combusted), and *A* is the area burned (m$^2$/unit time).

The sensible heat release *S* (J/unit time) of the same surface fire:

$$S = HmcA,$$

where *H* is heat of combustion (J/kg) and all other variables are previously defined.

The fuel load *m*, combustion completeness *c*, and area burned *A* are common to the calculation of *E* and *S*. In practice, estimates are readily available for the fuel consumed *F* which is equivalent to *mc*. As we discuss below *A* can be estimated from space-borne data that approximately dates the burning by locating the occurrence of rapidly changing daily surface reflectance time series data (http://modis-fire.umd.edu/Burned_Area_Products.html). For the other variables we have to rely on *in situ* measurements collected over different campaigns.

**MODIS burned area product**

We used the MODIS collection 5 level 3 monthly tiled product MCD45A1 that are gridded at 500m, unless otherwise stated, which contains the Julian day for the burning of each 500 m pixel. For each individual fire scenario we picked the nearest MODIS tile. For quality assurance, we retained pixels that were the most confidently detected and pixels where backward and forward directions in time predict the same change.

**Study Biomass Burning Scenarios**

We selected three surface fire scenarios during which there is substantial evidence of vertical transport of emissions to the UT: 1) Victoria, Australia, February 2009; 2) Siberia, July 2006; and 3) Borneo, October 2006. For each fire we provide the background that led up to the fire and the data used to quantify associated emission and heat release for consecutive days of the fires (1 for scenario 1, 2 for scenario 2, and 2 for scenario 3). The 5 scenarios are summarized in Table 1 and described below. All gridded emissions are reported here on a regular 2x2 km grid. In the absence of additional information, we assume that emissions are constant for the duration of the fire. For Victoria, we have enough information to approximate the evolution of the fire front (this will be done as part of the modeling task).

*Scenario 1: Victoria, Australia, February 2009*

Southeastern Australia experienced an extreme heatwave with record breaking temperatures during late January and early February 2009, preceded by severe drought [National Climate Centre, 2009]. The drought added to the dead, dry, woody biomass in forests and parks. The heatwave, noted for its length, had two acute stages: from 28 to 31 January and from 6 to 8 February. The state of Victoria was most affected during the second stage, on 7 February. The extended heatwave led to drying out of live plants increasing their combustibility.

Extreme meteorological conditions: high temperatures (max. 46°C), very low humidity (< 10%), and strong winds (50–60 km/hr), together with very dry fuels resulted in severe bushfires that burned an area of about 3,000 $km^2$ just on Saturday 7th February ("Black Saturday") [Tolhurst 2009]. A pyrocumulus cloud developed in the evening of 7 February above the Kilmore East fire, with cloud top estimated to be at about 8.5 km above ground level. Pyrogenic emissions were lofted rapidly into the free troposphere and were observed a few days later over the Pacific at altitudes of up to about 20 km by CALIPSO and in mid-April in the Antarctic stratosphere.

For this study we focused on the largest fire, the Kilmore East fire, that burned 85 km north of Melbourne and was caused by a failure of electrical powerlines. A total area of about 1,250 $km^2$ was burned [Royal Commission, 2010], most of it (1,150 $km^2$) on 7 February [Tolhurst, 2009]. On the 7 February, the day we have chosen to simulate with our model, calculations that supported the Royal Commission on the fires suggest that the total heat output of the fire was 53 PJ (P = Peta = $10^{15}$) [Tolhurst, 2009]. We found that the Kilmore East fire burned predominantly in the mountain forest. The resulting emission of 1.4 Tg C is consistent with the fuel load $m$ of 40t/ha reported from Mt Disappointment and a combustion efficiency $c$ of 0.5 based on data provided by the Global Fire Emission Database. For this scenario we assume a heat of combustion H of 18.7 MJ/kg (M = Mega = $10^6$) [Trentmann et al, 2006] and a carbon content $f$ of 0.48 kg C/kg dry fuel [van der Werf, 2010]. Based on the estimated heat output we estimate a total emission of 1.4 Tg C (T = Tera = $10^{12}$). Figure 1 shows the spatial distribution of the source on the high resolution model grid.

Our initial calculations used the MODIS 500 m burned area product (described above) but we found that the estimated area was only a small fraction[1] (5%) of the estimated area based on fire modelling and ground validation sites that supported the Royal Commission report on the Victoria fires (Figure 1). Because we had arguably more reliable data from the report, we used the fire distribution determined by the fires spread model used in the report [Tolhurst, 2009].

[1] We followed this up with relevant MODIS investigators at NASA GSFC but we did not receive a response. We believe these data are likely more reliable on longer than daily timescales which allows other researchers to infer emission inventories, e.g., the Global Fire Emission Database.

*Scenario 2: Siberia, Russia, July 2006*

Siberian wildfires are widespread during northern hemisphere summertime, exhibiting substantial year to year variability. We studied fires during July 2006 when fire activity was particularly large. Vertical transport of fresh biomass burning emissions was observed by CALIPSO, TES and MLS for that month [Verma et al, 2009; Gonzi and Palmer, 2010].

For our high-resolution atmospheric transport simulations, we selected two days, 23 and 27 July 2006, with large forest fires burning around (106°E, 63.5°N) and (116.5°E, 56.25°N), respectively. MODIS estimated burned areas of 55 and 25.5 $km^2$ for the selected times and regions (Table 1). We have estimated a total carbon release of 0.2 Tg for the 23 July fires and 0.1 Tg for the 27 July fires, and a heat output of 6.3 and 3.5 PJ, respectively, based on carbon consumption estimates from severe fire in northern taiga and boreal mountain forests [Soja et al, 2004]. Figure 2 show the spatial distribution of the two fire sources on the high resolution model grid.

*Scenario 3: Borneo, Indonesia, October 2006*

Large fires (the largest since 1997) associated with a weak El Niño burned across Indonesia during the dry season (August–October) of 2006. Emissions lofted to the UT were observed, e.g., by many of the orbiting satellites ACE-FTS [Lupu, 2009], TES [Logan et al, 2008], MLS [Chandra et al, 2009], AIRS, and MOPITT.

We encountered a large underestimation of burned area using the MODIS daily 500-m burned area product for Borneo, similar to the Victoria fires (see above). We cross checked the burned area product over Borneo with MODIS active fires (hotspots) and found large regions with fires but no burned area pixels. Consequently, for Borneo we decided to use the monthly burned area from the Global Fire Emission Database v3 (see Footnote 1), described on a 0.5 degree x 0.5 degree spatial grid, weighted by the number of daily hotspots in order to approximate the daily burned area; we acknowledge the shortcomings of using firecounts for this purpose [Mota et al, 2006]. For this calculation we use only high-confidence pixels based on the prescribed quality assurance flags provided by the developers. We acknowledge that burned area does not scale linearly with the number of active fires, but this error is not likely to be very important. To test this hypothesis, we calculated the monthly burned area per hotspot by dividing the GFEDv3 area by the total number of hotspots in a month. We found that this value varied only between 27 and 36 ha for Borneo for August–November 2006, suggesting a reasonably robust method.

We selected two days for simulation based on the number of MODIS firecounts: 30 September and 30 October 2006. Assuming average carbon emissions of 169 Mg C $ha^{-1}$ [Heil, 2007], we estimate for southern Borneo a total release of 6.7 Tg C for 30 September and 16.2 Tg C for 30 October. Energy released from combustion can be lost by conduction, radiation and convection. We assume that energy released from peat is not available for convection and that peat contributes 60.5% to the total carbon emissions [Heil, 2007]. The heat released during the two days amounts to 103 and 249 PJ, if assuming a standard heat of combustion of 18.7 MJ $kg^{-1}$. Figure 3 show the spatial distribution of the southern Borneo fires on the high resolution model grid.

## Comparative study of fires and subsequent emissions

Table 1 and Figure 4 provide a comparison of emissions from the individual fires. Broadly, the three study fires span very different fire scenarios to test PREMIER, reflecting differences in the fuel loading and the area burned. The two gases with the largest emissions are $CO_2$ and CO, as expected. The next largest emissions, which vary in relative importance according to the fires studied, are from $CH_4$, methanol ($CH_3OH$), formaldehyde (HCHO), and ethane ($C_2H_6$). The relative importance is similar for Victoria and Siberia, but the amount of material emitted per unit space and time is greater for Siberia, reflecting the greater fuel loading at this location (Table 1). Borneo has a much higher proportion of $CH_4$ due to the understorey burning of peat which is rich in $CH_4$. The amount of material emitted for this fire per unit space and time is almost three times that of Siberia.

Figure 5 shows the distribution of fire emission for Borneo on the two study dates. On both dates the fire is widespread but there are regions with higher emissions that reflect gradients in the fuel loading and the fire activity. These two dates also serve to demonstrate the importance of temporally resolving fire emission, with October 30th associated with much larger fires resulting in twice the amount of carbon released into the atmosphere.

## References

Gonzi, S., and Palmer, P. I.: Vertical transport of surface fire emissions observed from space, J. Geophys. Res., 115, D02306, 2010, doi:10.1029/2009JD012053, http://dx.doi.org/10.1029/2009JD012053.

Heil, A.: Indonesian Forest and Peat Fires: Emission, Air Quality, and Human Health, PhD thesis, Max Planck Institute for Meteorology, Hamburg, Germany, 2007, http://www.earthsystemschool.mpg.de/fileadmin/user_upload/Documents/Theses/34_Thesis_Heil.pdf.

Lupu, A., et al.: Hydrogen cyanide in the upper troposphere: GEM-AQ simulation and comparison with ACE-FTS observations, Atmos. Chem. Phys. 9, 4301–4313, 2009. doi:10.5194/acp-9-4301-2009, http://dx.doi.org/10.5194/acp-9-4301-2009.

Mota, B. W., et al, Screening the ESA ATSR-2 World Fire Atlas (1997-2002), Atmos. Chem. Phys., 6, 1409-1424, 2006.

National Climate Centre: The exceptional January-February 2009 heatwave in southeastern Australia, Bureau of Meteorology, Special Climate Statement 17, 2009, http://www.bom.gov.au/climate/current/statements/scs17d.pdf.

Royal Commission: The 2009 Victorian Bushfires Royal Commission Final Report, July 2010, http://www.royalcommission.vic.gov.au/Commission-Reports/Final-Report.

Soja, A. J., W. R. Cofer, H. H. Shugart, A. I. Sukhinin, P. W. Stackhouse Jr., D. J. McRae, and S. G. Conard, Estimating fire emissions and disparities in boreal Siberia (1998–2002), *J. Geophys. Res.*, 109, D14S06, doi:10.1029/2004JD004570, 2004.

Tolhurst, K.: Report on the Physical Nature of the Victorian Fires occurring on 7th February 2009, 2009, http://www.royalcommission.vic.gov.au/getdoc/5905c7bb-48f1-4d1d-a819-bb2477c084c1/EXP.003.001.0017.pdf.

Trentmann, J., Luderer, G., Winterrath, T., Fromm, M. D., Servranckx, R., Textor, C., Herzog, M., Graf, H.-F., and Andreae, M. O.: Modeling of biomass smoke injection into the lower stratosphere by a large forest fire (Part I): reference simulation, Atmos. Chem. Phys., 6, 5247-5260, doi:10.5194/acp-6-5247-2006, 2006.

van der Werf, G. R., et al.: Global fire emissions and the contribution of deforestation, savanna, forest, agricultural, and peat fires (1997–2009), 2010, doi:10.5194/acpd-10-16153-2010, http://dx.doi.org/10.5194/acpd-10-16153-2010.

Verma, S., et al., Ozone production in boreal fire smoke plumes using observations from the Tropospheric Emission Spectrometer and the Ozone Monitoring Instrument, *J. Geophys. Res.*, 114, D02303, doi:10.1029/2008JD010108, 2009.

**Table 1.** Assumed and derived quantities for individual fire scenarios.

| | Victoria[a] | Siberia #1 | Siberia #2 | Borneo #1 | Borneo #2 |
|---|---|---|---|---|---|
| Date | 7 February 2009 | 23 July 2006 | 27 July 2006 | 30 September 2006 | 30 October 2006 |
| Location | 144.5–146°E 37–38°S | 103–109°E 62–65°N | 113–120°E 54.5–58°N | 109–117°E 1–5°S | 109–117°E 1–5°S |
| Total area burned ($km^2$) | 1150.00[h] | 55.00[i] | 25.50[i] | 398.00[j] | 958.00[j] |
| Fuel consumption ($Mg\ ha^{-1}$) | 24.65 | 61.67 | 74.06 | 351.67 | 351.67 |
| Carbon consumption[b] ($Mg\ C\ ha^{-1}$) | 11.83 | 29.60[e] | 35.55[f] | 168.80[g] | 168.80[g] |
| Total dry matter burned (Tg) | 2.83 | 0.34 | 0.19 | 14.00 | 33.69 |
| Total carbon emission[b] (Tg C) | 1.36 | 0.16 | 0.09 | 6.72 | 16.17 |
| Total sensible heat (PJ) | 53.00[h] | 6.34[c] | 3.53[c] | 103.38[c,d] | 248.85[c,d] |
| *Emissions*[k] ($g/m^2/h$) | | | | | |
| $CO_2$ | 322.855 | 403.917 | 485.109 | 2450.802 | 2450.802 |
| CO | 21.770 | 27.236 | 32.711 | 244.621 | 244.621 |
| $CH_4$ | 0.986 | 1.233 | 1.481 | 22.259 | 22.259 |
| NO | 0.700 | 0.876 | 1.052 | 3.312 | 3.312 |
| $SO_2$ | 0.205 | 0.257 | 0.309 | 1.040 | 1.040 |
| $CH_3OH$ | 0.369 | 0.462 | 0.555 | 2.908 | 2.908 |
| HCOOH | 0.500 | 0.625 | 0.751 | 1.656 | 1.656 |
| $C_2H_6$ | 0.151 | 0.188 | 0.226 | 1.761 | 1.761 |
| $C_2H_2$ | 0.053 | 0.067 | 0.080 | 0.589 | 0.589 |
| $C_2H_4$ | 0.252 | 0.315 | 0.378 | 2.840 | 2.840 |
| $C_3H_8$ | 0.052 | 0.065 | 0.078 | 1.526 | 1.526 |
| HCHO | 0.385 | 0.482 | 0.579 | 1.512 | 1.512 |
| HCN | 0.166 | 0.208 | 0.250 | 0.440 | 0.440 |
| $CH_3CN$ | 0.060 | 0.075 | 0.090 | 0.591 | 0.591 |
| ALD2 (Acetaldehyde and higher aldehydes)[l] | 0.201 | 0.252 | 0.302 | 1.279 | 1.279 |
| $C_5H_8$ | 0.021 | 0.026 | 0.032 | 0.023 | 0.023 |
| $CH_3COOH$ | 0.719 | 0.899 | 1.080 | 6.437 | 6.437 |
| ALKA (Higher alkanes)[l] | 0.091 | 0.113 | 0.136 | 0.409 | 0.409 |
| ALKE (Higher alkenes)[l] | 0.279 | 0.349 | 0.419 | 3.602 | 3.602 |
| AROM (Aromatics)[l] | 0.068 | 0.085 | 0.102 | 0.127 | 0.127 |
| Toluene | 0.221 | 0.277 | 0.332 | 1.089 | 1.089 |

| | | | | | |
|---|---|---|---|---|---|
| MEK (Acetone and higher ketones)[l] | 0.138 | 0.173 | 0.207 | 1.053 | 1.053 |
| MGLY (Glyoxal and methylglyoxal)[l] | 0.351 | 0.439 | 0.527 | 2.503 | 2.503 |
| HONO | 0.046 | 0.057 | 0.069 | 0.326 | 0.326 |
| Black carbon (aerosol) | 0.115 | 0.144 | 0.173 | 0.835 | 0.835 |
| Organic carbon (aerosol) | 1.877 | 2.348 | 2.821 | 6.301 | 6.301 |

[a]Kilmore East fire only; [b]Assuming a carbon content of 48% (van der Werf *et al.*, 2010); [c]Assuming a heat of combustion of 18.7 MJ $kg^{-1}$ (Trentmann *et al.*, 2006); [d]Calculated by assuming that energy released from peat is not available for convection and that peat contributes 60.5% to the total carbon emissions (Heil, 2007); [e]Carbon consumption for severe fire in northern taiga (Soja *et al.*, 2004); [f]Carbon consumption for severe fire in boreal mountain forest (Soja *et al.*, 2004); [g]Heil (2007); [h]Tolhurst (2009); [i]MODIS 500-m burned area product; [j]Estimated from MODIS daily active fire product and monthly carbon emissions from GFEDv3 (van der Werf *et al.*, 2010); [k]Emission factors from Andreae & Merlet (2001) and Andreae, personal communication (2006); emission fluxes calculated by assuming a total fire duration of 12 hours for the Kilmore East fire and 1 day for all others; [l]Lumped species in GEM-AQ chemistry mechanism (Kaminski *et al.*, 2008)

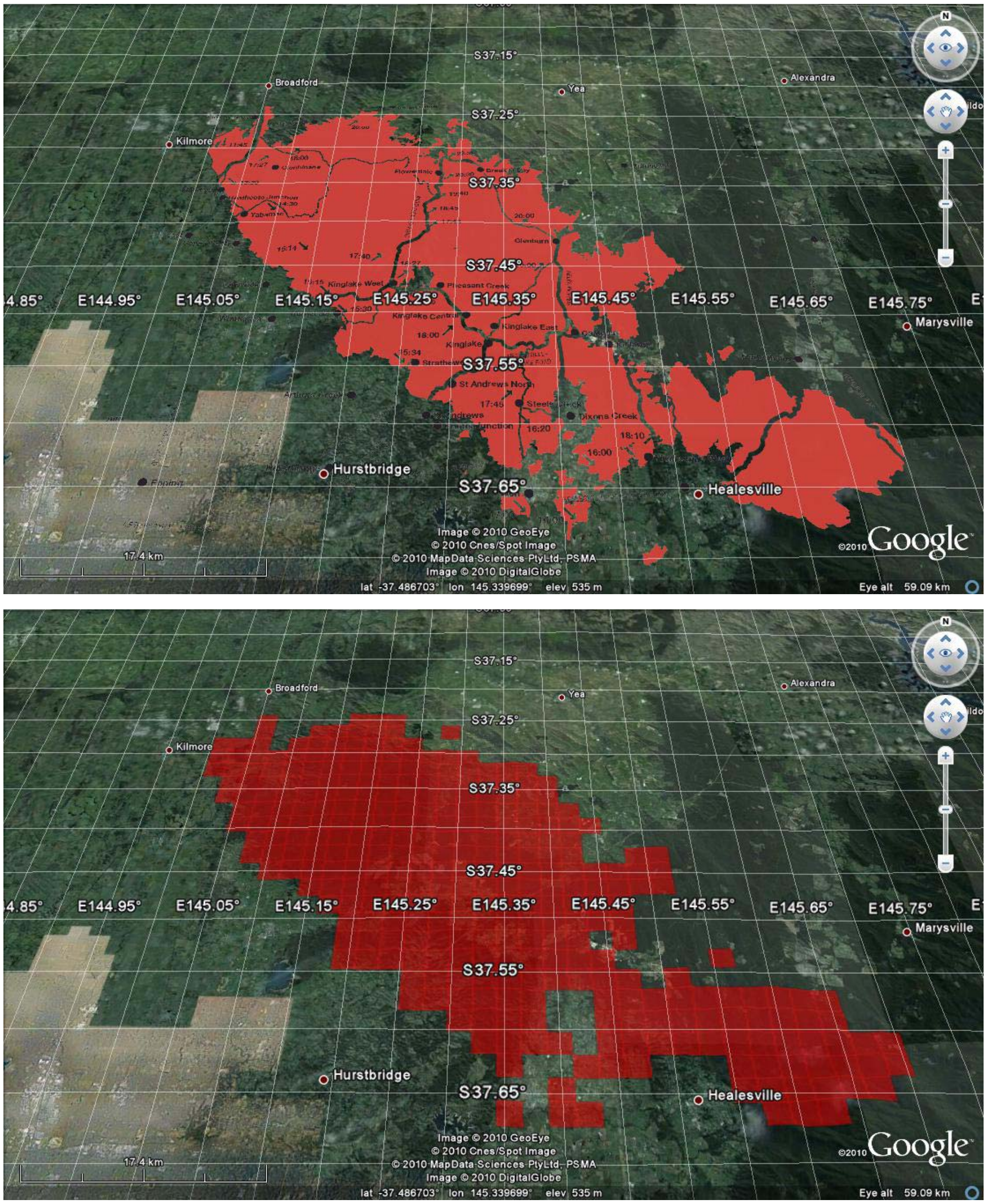


**Figure 1 Distribution of active fires during the Kilmore East Fire, Victoria Australia, February 7th 2009, determined using (top) the fire spread model used by the Royal Commission [Tolhurst, 2009] and (bottom) subsequently regridded onto a regular 2x2 km spatial grid.**

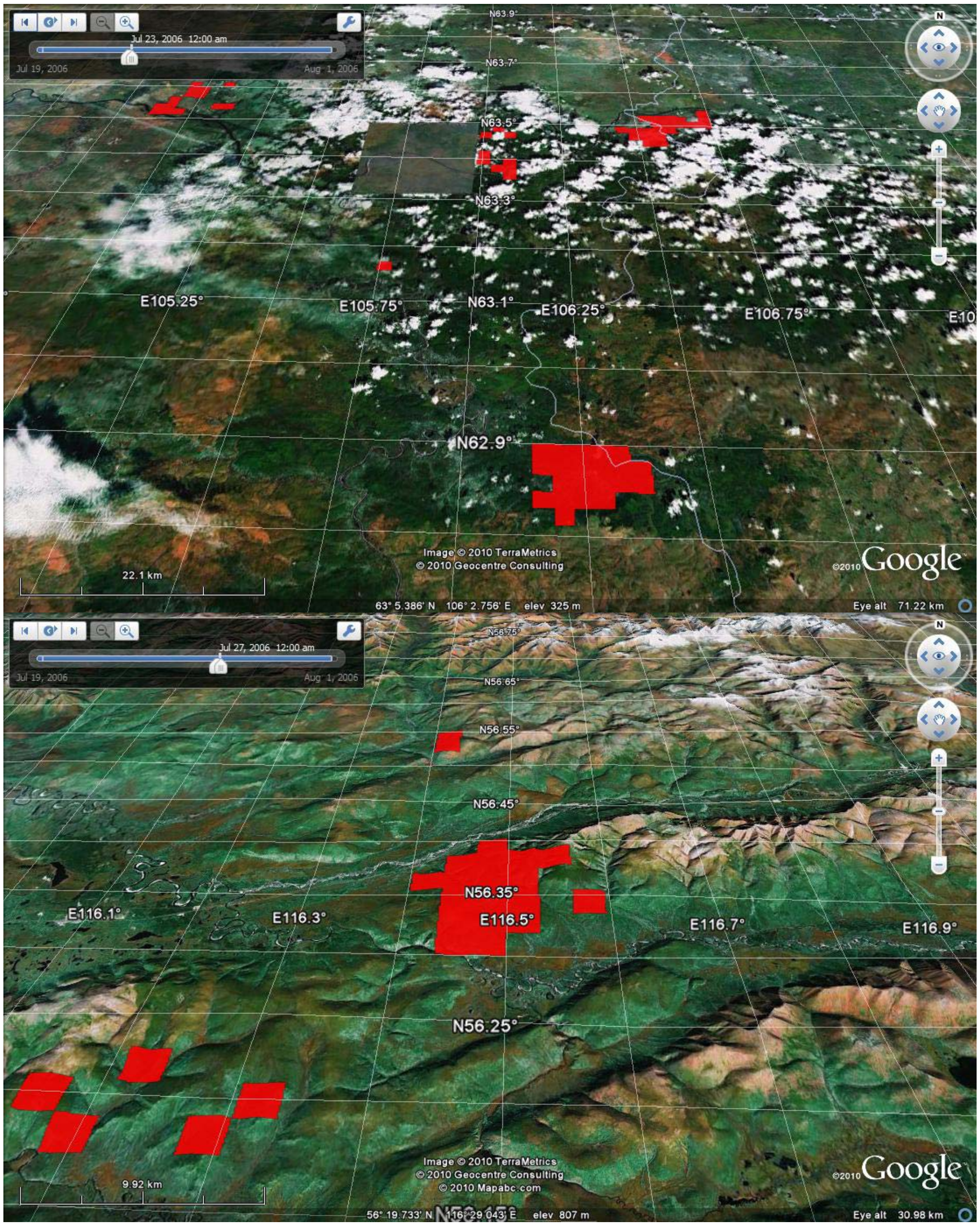


**Figure 2 Distribution of active fires over Siberia on a regular 2x2 km spatial grid for the 23rd (left) and 27th (right) July 2006 determined using the 500-m MODIS burned area product.**


**Figure 3 Distribution of active fires over Borneo on a regular 2x2 km spatial grid during the 30th September 2006 (left) and the 30th October 2006 (right) determined from the relevant monthly Global Fire Emission Database values scaled by MODIS firecounts.**

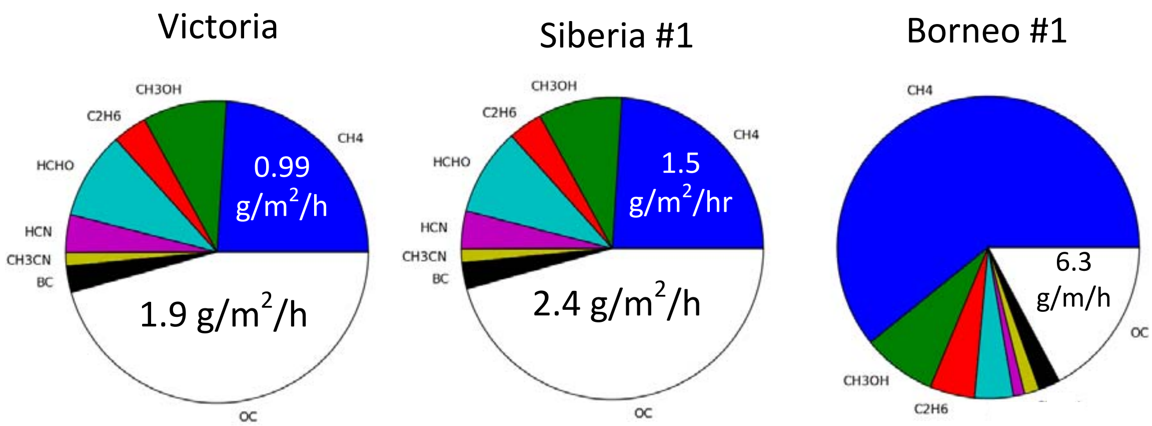


**Figure 4 Emission estimates (g/m$^2$/h) from the three candidate fires chosen as part of the PREMIER impact study, based on fire characteristics shown in Table 1. Emission factors are from Andreae & Merlet (2001) and Andreae, personal communication (2006).**

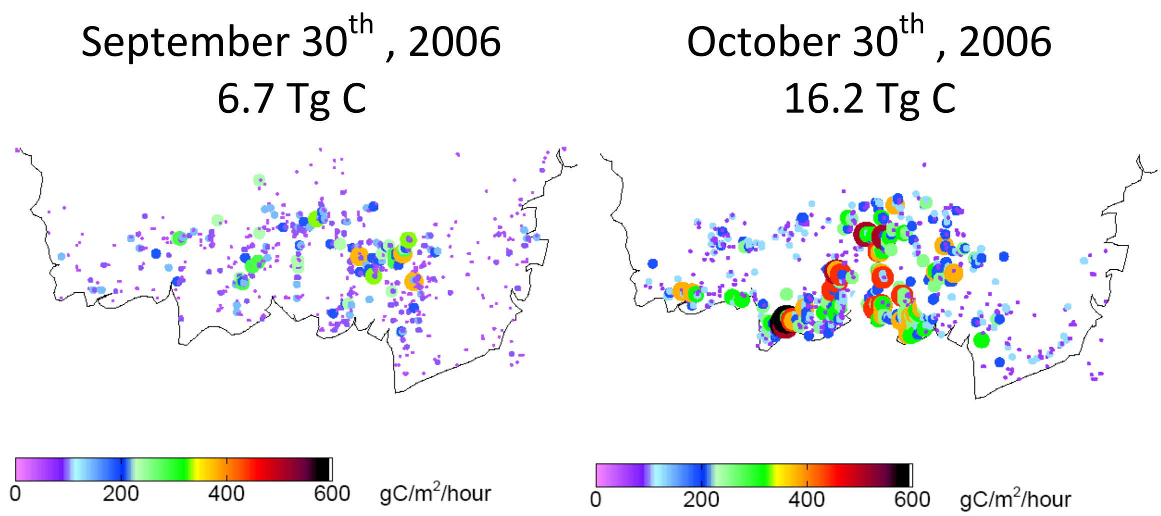


**Figure 5 Example distributions of fire emissions (gC/m$^2$/h) for Borneo described on a regular 2x2 km$^2$ grid on September 30th 2006 and October 30th 2006. To help interpret the plot, the size of the circles denotes the magnitude of the emissions. Inset to each panel is the total carbon emitted for that day.**